

Versatile methodology for the synthesis of stable magnetic SERS encoded clusters for sensing applications

SUPPLEMENTARY INFORMATION

*Francisco J. Caparrós,^a Paulo Alexandre Gomes,^a Manuel García-Algar,^a María Rivero,^a
Samantha Grand,^a Mario Borràs,^a Juan Sagales^b and Sara Gómez-de Pedro^{*a}*

^a Medcom Advance, Carrer de Marcel·lí Domingo 2-4, Edifici N5, 43007 Tarragona, Spain

^b MedcomTech, Viladecans Business Park, Edificio Australia, Carrer Antonio Machado 78-80,
08840 Viladecans, Barcelona, Spain

*E-mail: saragomez.medcomadvance@gmail.com

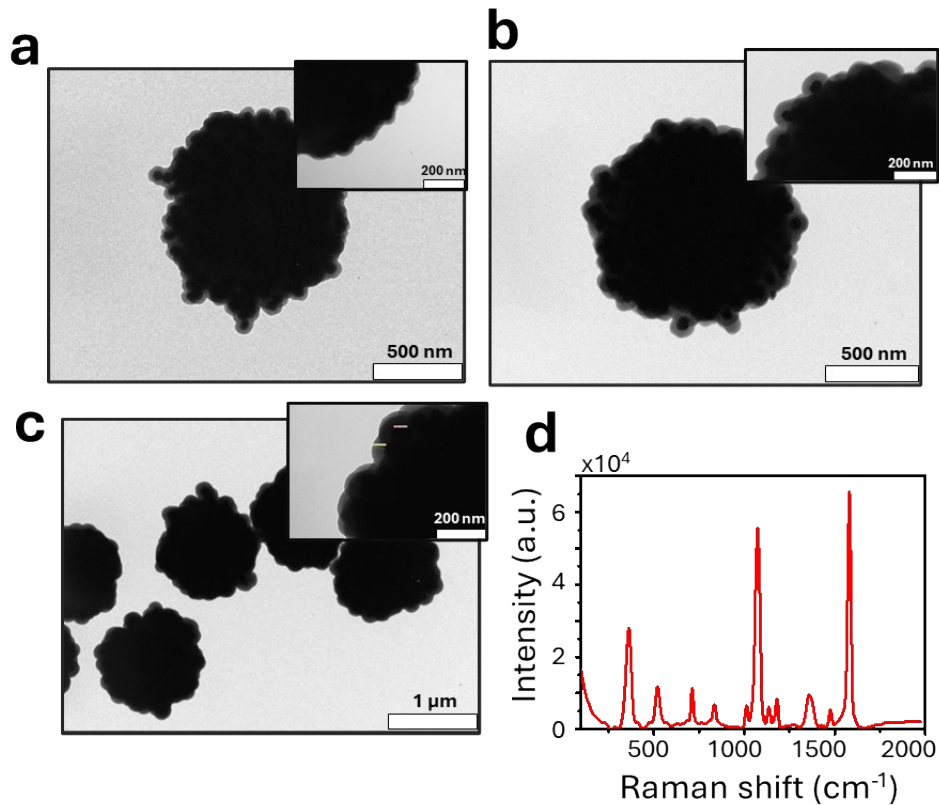


Fig. S1. Silica coated magnetic SERS tags, with 1.0 μm core size diameter and conjugated with 72 nm silver nanoparticles. A-C) TEM images of the magnetic tags with one, two and three SiO_2 layers, respectively. Amplification images are shown, where the encoded silver nanoparticles can be well distinguished. D) SERS spectrum for the three SiO_2 layers coated tags (average from at least 24 single particles).

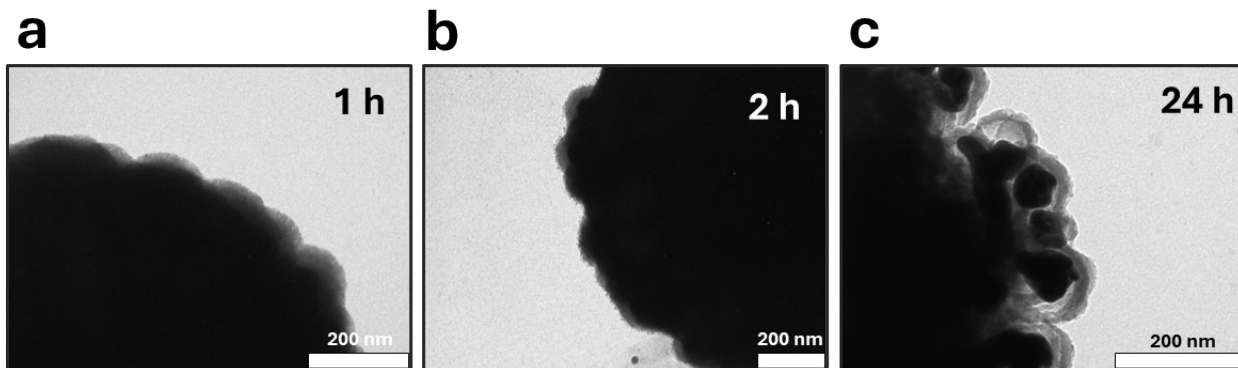


Fig. S2. Effect of water as solvent over time on the SiO_2 coated magnetic clusters. As example, magnetic clusters of 1.0 μm core size were used, conjugated to 72 nm silver nanoparticles encoded with MBA as Raman label.

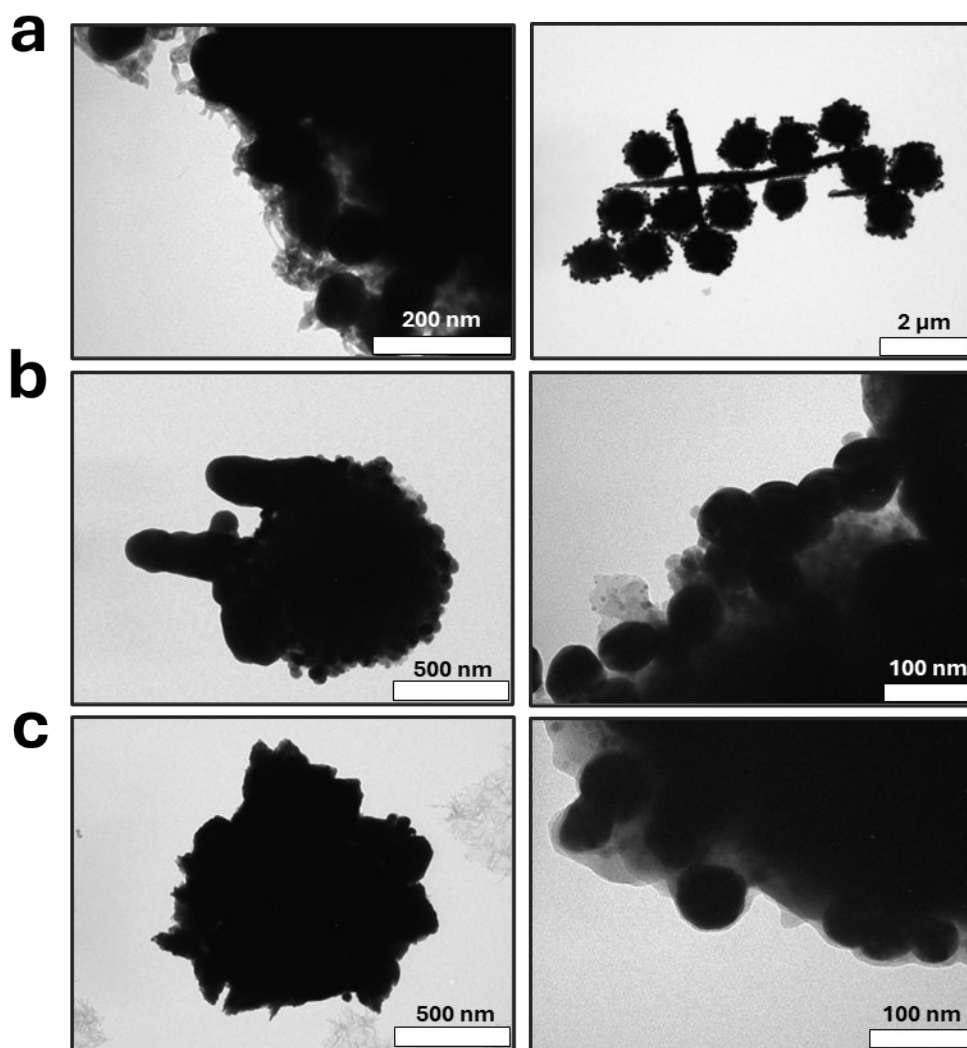


Fig. S3. TEM images of ZnO coated magnetic SERS tags, with 1.0 μm core size diameter and conjugated with 72 nm silver nanoparticles. External coating was synthesized using A) ZnO-protocol 1, B) ZnO-protocol 2 and C) ZnO-protocol 3.

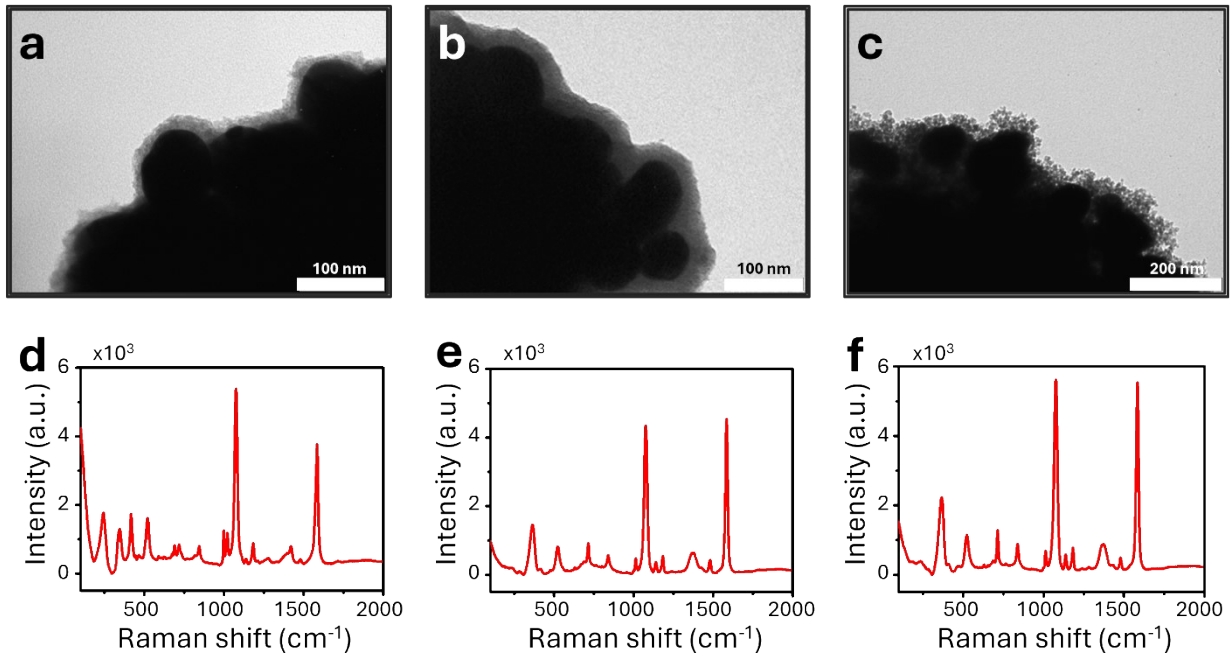


Fig. S4. TiO_2 coated magnetic SERS tags, with $1.0 \mu\text{m}$ core size diameter and conjugated with 72 nm silver nanoparticles. A-C) TEM images of the magnetic tags, TiO_2 coated using TiO_2 -protocol 1, 2 and 3, respectively. Amplification images are shown. D-F) SERS spectra for the three types of TiO_2 layers tags.

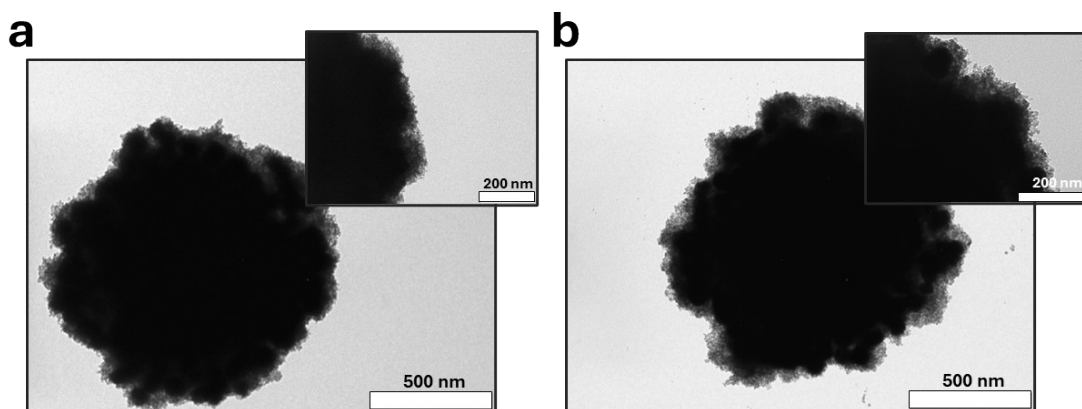


Fig. S5. Effect of water as solvent on TiO_2 coated magnetic SERS tags, with $1.0 \mu\text{m}$ core size diameter and conjugated with 72 nm silver nanoparticles. A) TEM image of freshly prepared tags B) TEM image of same particles after four months in water. Amplification images are also shown.

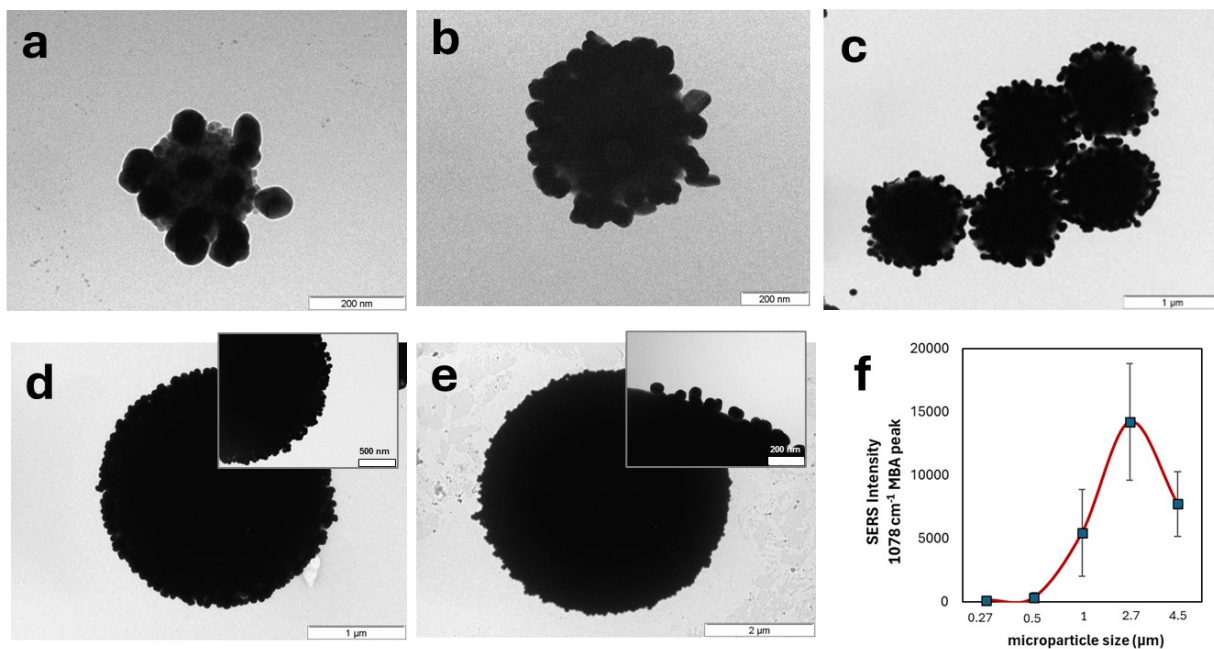


Fig. S6. A-E) TEM images from conjugated magnetic clusters with diverse core sizes encoded with 4-MBA; a) 0.27 μm , b) 0.54 μm , c) 1.0 μm , d) 2.8 μm , with amplified image, e) 4.5 μm , with amplified image. f) Effect of SERS intensity on the different size of magnetic clusters, conjugated with 72 nm silver nanoparticles 4-MBA encoded. Maxima intensity (1072 cm^{-1}) are the average value for at least 24 different spectra of single particles.

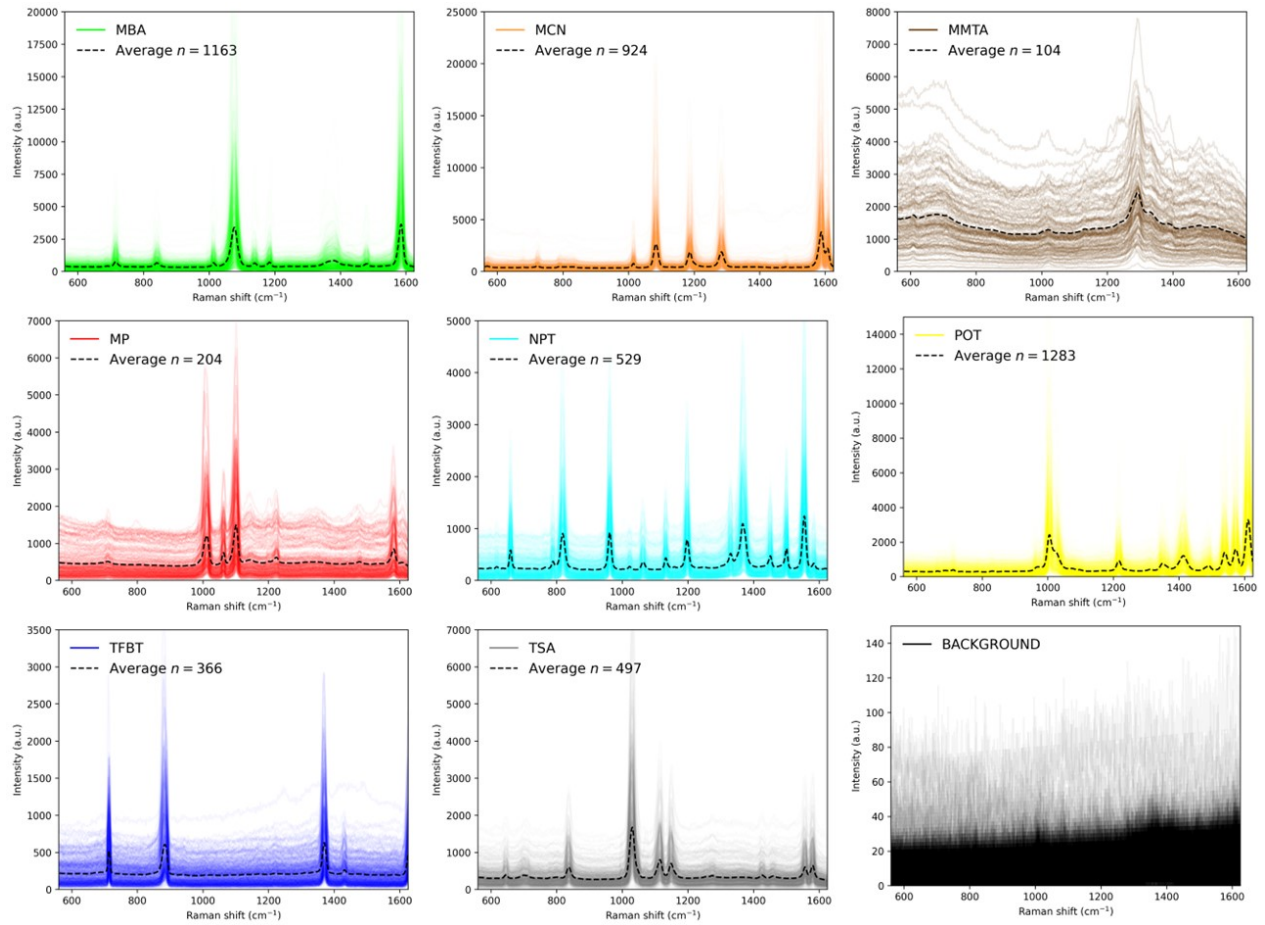


Fig. S7: Raw Raman spectra used for the SOM training, outlining the variability of each particle, the average spectra and the Raman shift considered.

DATA ANALYSIS:

For the Raman analysis, an algorithm based on Artificial Neural Networks (ANN) was used. The ANN can be effectively trained to distinguish multi-class Raman samples by running many combinations of spectra data. Self-Organizing Maps (SOM) is a custom ANN which has proved successful results when applied to Raman data.¹ SOM can reduce the dimensionality of the Raman data. The map organizes spectra of the same class into the same region as clusters. Depending on the proximity of other clusters, the spectra are more similar or different from each other. In a SOM map, each grid element (hexagon) is represented as a neuron that only accepts spectra like the ones the neuron was trained on, thus providing information related to the different class fingerprints and similar classes based on proximity. SOM has been implemented using the MiniSOM² module version = 2.3.1, which handles the entire SOM implementation and mathematics in Python, and later adapted by us for our needs.

Raman spectra were sampled from different synthesized magnetic SERS Tags. By acquiring large Raman maps from various batches of particles, a large dataset was obtained. Only the most intense spectrum was stored per particle, amounting to the total sample size described (Fig. S7). Due to an imbalance in the sample size, a total of 200 spectra were randomly selected from each dataset for training the SOM model. The lower spectra number of the MMTA functionalization did not affect the model's accuracy, as all spectra have high intensity and are easily distinguishable among them. Fig. 6A shows the normalized average spectra (after cosmic ray removal, baseline subtraction and normalization) representative of each functionalization to be identified. The Raman measurements were acquired at 0.5 seconds and 10% laser power setting using the 785nm laser in the RA806 Renishaw system. The SOM model shows a dramatic improvement over the manual peak selection, offering a better presentation of the data, clearer insight, and greater classification accuracy.

Fig. 6B shows the projection of the hyperspectral data set into 2D space showing a clear separation of the spectra data from the eight different functionalization classes and the background class, arranged as in a 20 x 20 neuron grid and its classification score (Table S1). Each neuron (hexagon) is populated by colored dots representing a spectrum from the training data activated by that neuron. Neurons that do not activate any of the training data are shown in greyscale and have no colored dots. For each class, there is a clearly defined block of neurons with the same functionalization. Most of the background spectra are located centrally at the boundary between classes, meaning that some of the spectra from the functionalization's are relatively noisy and thus share the interface with the background class.

Table S1. Classification report for the SOM analysis.

| Label | Precision | Recall | F1-score | Support |
|--------------|-----------|--------|----------|---------|
| MBA | 1.00 | 1.00 | 1.00 | 50 |
| MCN | 1.00 | 1.00 | 1.00 | 50 |
| MMTA | 1.00 | 0.96 | 0.98 | 26 |
| MP | 0.76 | 1.00 | 0.86 | 50 |
| NPT | 1.00 | 1.00 | 1.00 | 50 |
| POT | 1.00 | 0.98 | 0.99 | 50 |
| TFBT | 1.00 | 0.98 | 0.99 | 50 |
| TSA | 1.00 | 1.00 | 1.00 | 50 |
| BACKGROUND | 1.00 | 0.74 | 0.85 | 50 |
| Accuracy | | | 0.96 | 426 |
| Macro avg | 0.97 | 0.96 | 0.96 | 426 |
| Weighted avg | 0.97 | 0.96 | 0.96 | 426 |

The trained SOM model allows us to perform automated classification of Raman spectra and assign them to a particular disease state. By looking up the model class of the neuron activated for a test sample, the proper classification for a spectrum can be obtained. We ran a multiplex experiment on a sample with all different labels (*MBA*, *MCN*, *MMTA*, *MP*, *NPT*, *POT*, *TFBT*, *TSA*), outputting the SOM activation map (**Fig. S8B**) overlapped with the white light image (**Fig. S8A**) of the measured region resulting in the colored white light image (**Fig. 6C**). Here, the trained model can easily identify the eight different labels, and by manual inspection (**Fig. S8C**), we confirmed that all classifications were correct. Moreover, statistical information can be obtained regarding the amount of a specific label present in the sample (**Fig. 6C, inset**).

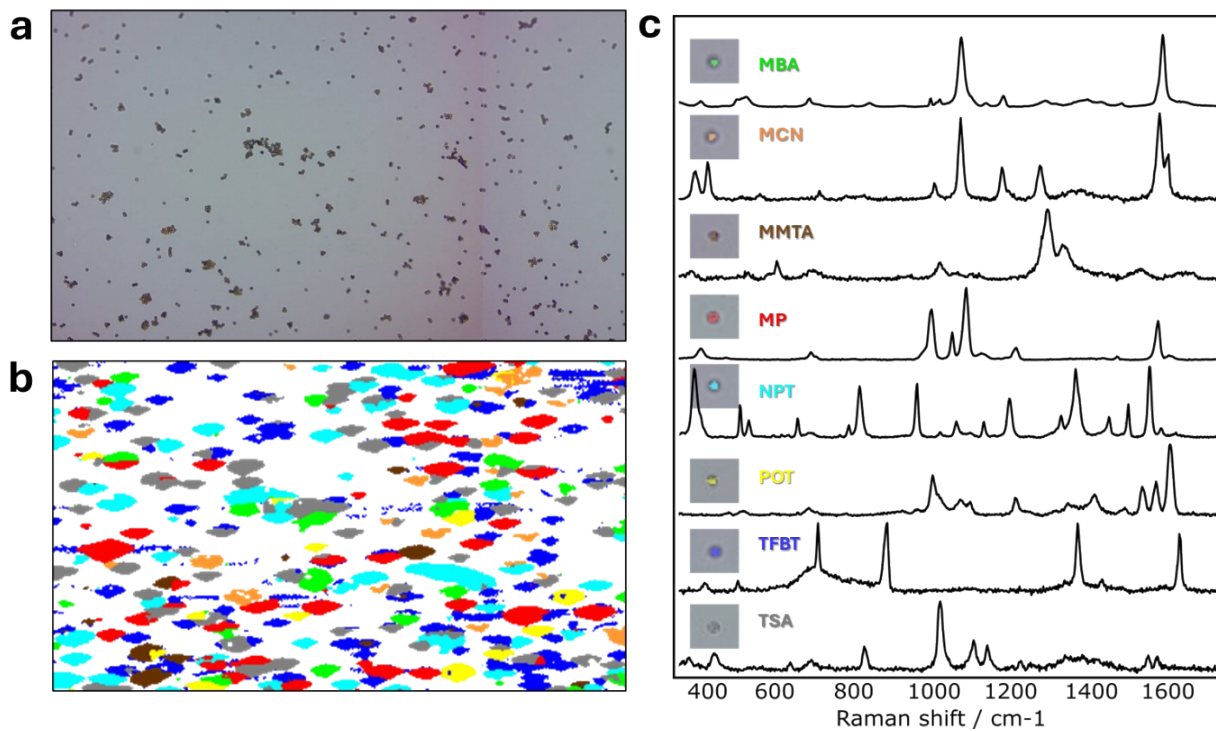


Fig. S8. A) White light image of the mixed magnetic SERS Tags. B) SERS map for the same Tags. C) Individual spectra from single Tags. Ground Truth done by manually adjusting all the peak parameters.

For testing the SOM model accuracy, the 200 spectra per class dataset was split into 75% training (150 spectra) and 25% testing (50 spectra), obtaining the classification report in **Table S1**, where the output accuracy score was 96%, showing the good classification ability of the model. The lower values for precision in *MP*, lower recall for the *BACKGROUND*, and both with lower F1-score can be explained by the high variability in the raw Raman spectra (**Fig. S7**) and potentially some kind of commonality of peaks between *MP* and *MBA*, *MCN*, *POT*, and *TSA*. The fact that they have one similar peak range in $1065\text{-}1088\text{cm}^{-1}$ can lead to this kind of variability in the results if the signal intensity is low. However, the important parameter is the model's accuracy, which is very high, indicating that the model has been properly trained.

1. C. Banbury, R. Mason, I. Styles, N. Eisenstein, M. Clancy, A. Belli, A. Logan, P. Goldberg Oppenheimer, *Sci. Rep.*, 2019, **9 (1)**, 10812.
2. G. Vettigli, *MiniSom: minimalistic and NumPy-based implementation of the Self Organizing Map*. <https://github.com/JustGlowing/minisom/> (accessed 2024-06-26).